The character of two-phase gas/particulate flow equations

A. D. Fitt

Faculty of Mathematics, University of Southampton, Southampton, UK

In classical (single-phase) fluid mechanics, it is a matter of experience that, away from flow boundaries, inviscid models often give excellent results. For time-dependent two-phase flows, an attractive possibility is to likewise ignore viscosity in the "mainstream" flow. However, such equations are generally not hyperbolic, and possess complex eigenvalues. This creates severe technical difficulties as the initial value problem is then ill-posed, and serious numerical problems that may render accurate computation impossible. This ill-posedness has been the subject of heated controversy, but the conclusion is clear. Doubt remains over the correct equations even for simple two-phase flows.

Complex characteristics arise as a result of multiphase flow averaging, and the consequent omission of important physical terms. With care, however, these effects may be reintroduced into the equations. Using such an approach, the specific case of gas/particulate two-phase flow is considered. The aim is not to propose a definitive, demonstrably "correct" system of equations for unsteady two-phase gas/particulate flow, the assumptions made are too general and specific cases must be treated on their individual merits. Rather a methodology of analysis is illustrated and qualitative results concerning the nature of added terms in the equations are obtained. The effect of each term and also of combinations of terms is studied, and general conclusions are drawn concerning the hyperbolicity of the equations.

Keywords: two-phase flow, gas/particulate flow, nonhyperbolicity, ill-posedness, flow modelling, hyperbolicity maps

1. Introduction

Two-phase flows occur in many industrial, engineering, and defense-related processes. Much literature exists concerning models for such flows that employ averaging to describe the motion. The multitude of different phasic material combinations that have been considered using such flow models includes bubbly gas/liquid flow,[1] stratified and annular gas/liquid flows,[2] and particle/liquid flows,[3] but the two-phase flows that we wish to specifically consider in this study are of another type, namely gas/particulate flows. In this instance, the continuous phase (designated phase 1) is assumed to be a gas and the dispersed phase (phase 2) is composed of solid particles. For the present we make no stipulations concerning the number or size distribution of the particles. This allows us to consider flow problems ranging from the motion of "dusty" gases where the particles are negligible in volume fraction concentration to flows where there may be areas consisting solely of particles, present in a conglomeration of some sort. It is perhaps worth mentioning that the original problem that suggested the need for a study of the present form was the classical internal ballistics problem of determining the flow inside a tank gun (see, for example, Gough and Zwarts[4]). Here the solid phase is composed of reactive propellant granules that are free to move around in the flow. As the flow evolves, the burning grains are transformed into phase 1, the surrounding gas, which is at high pressure and temperature. Throughout the discussion below, the work will be given a specific context by referring to the internal ballistics problem. The discussion is, however, of a general nature and the changes required to treat other gas/particulate flows would be small.

A serious problem in the development of continuum two-phase flow models has been the complication that in many circumstances the proposed conservation laws have been ill-posed in the sense that the system possesses complex characteristics. This fact, which seems to have been noted first by Gidaspow,[5] renders the numerical solution of such problems extremely difficult.[6] The numerical assessment of such models was considered by Stewart and Wendroff.[7] A common assumption of early two-phase flow models was that the pressures in both phases were identical. The flaw in this line of reasoning is apparent when we consider the flow of gas around a single solid sphere, for example: The pressure on the surface of the sphere is patently

Address reprint requests to Dr. Fitt at the Faculty of Mathematics, University of Southampton, Southampton SO9 5NH, UK

Received 12 March 1992; revised 19 October 1992; accepted 5 November 1992

not the same as the free stream pressure. Various "fixes" of the standard models have been proposed, some involving two-pressure models and others more exotic assumptions. Stuhmiller[8] included drag and interfacial pressure terms, deriving a model having real characteristics under certain circumstances, whereas Prosperetti and Van Wijngaarden[2] were able to propose a model with real characteristics using certain compressibility assumptions. Ransom and Hicks[9] considered the Riemann problem at the interface between the two phases in annular flow and were able to propose a two-pressure model that included a void fraction propagation equation. This was derived largely from intuitive physical arguments, but rendered the system totally hyperbolic. Such models provide partial solutions to the ill-posedness problem, but suffer from the drawback that being by their very nature fixes for specific cases, it is hard to justify them using rational averaging and asymptotics on generic conservation laws. Rather, extra equations have been added piecemeal to ensure real characteristics.

A more general approach was pioneered by Drew[10] and Ishii,[11] and developed and refined for two-phase flow.[12,13,14] The general philosophy was to write down generic conservation laws, carry out the averaging processes carefully, and finally propose a model that included as many physical effects as possible. Attention was then focused on the specific two-phase flow regime that was to be studied, and submodels developed for quantities such as the lift, drag, and interfacial terms. A careful nondimensionalization was then required to identify the leading order terms and important effects before the final system of "working" equations could be proposed. Although it is undoubtedly true that this approach to the problem is complicated and time-consuming, such a method will be adopted in the present study. To proceed in this way may be thought of as an acknowledgement that, although it would be very convenient to write down the correct terms for inclusion in the model in a more ad hoc fashion, the problem is just too complicated and there are too many subtly competing effects to be able to do this with any guarantee of accuracy.

After the basic equations have been proposed, our aim is to indicate how the various submodelling tasks could be carried out, and then to examine in detail the effects of all the terms on the hyperbolicity of the system. In the past such an analysis would have involved prohibitive amounts of calculation, but the modern generation of symbolic algebra systems makes the task a realistic possibility. As far as previous studies looking at the effects on the well-posedness of the added terms in the equations are concerned, only the virtual mass terms seem to have received much consideration up to the present time. An examination of the effects of virtual mass was undertaken by Drew, Cheng, and Lahey.[15] Under the assumption that any virtual mass terms must be objective, a general form of the virtual mass term was derived. The relevance of such modelling to the hyperbolicity of the conservation laws was not explored, however. An alternative strategy for considering virtual mass effects in liquid/bubble flows was considered by Cook and Harlow.[16] Their three-phase treatment divided the flow into bulk liquid, bubble vapor, and liquid associated with virtual mass inertia regions. By this means, they were able to obtain a form for the virtual mass expression that did not involve any unknown coefficients, while still ensuring objectivity. The expression is rather complicated, however, and again the effect of the submodel on the general system of equations was not pursued. Constitutive relations for the lift force on the particulate phase have also been examined[17] and details of constitutive laws for some flow regimes derived by other authors were summarized by Drew,[13] but once again no examination of their effects on the hyperbolicity of the system was undertaken.

1.1. Ill-posedness and nonhyperbolicity

Before proceeding with the development of the general equations, it is worthwhile to briefly detail the reasons why we consider the presence of complex eigenvalues so undesirable. Elliptic equations are known to describe a wide variety of physical phenomena (electrostatics, elasticity, steady inviscid incompressible irrotational fluid flow, etc.) with great accuracy, but invariably in these models time does not appear as an independent variable. The typical elliptic system comes about as a result of an evolutionary process that has reached a steady state; the problem is to determine this steady state. Suitable boundary conditions normally consist of the specification of data over the whole of the boundary of the solution region. For evolutionary problems, the situation is fundamentally different. Time is a distinguished variable that may run only in one direction (witness the well-known ill-posedness of the "backward" heat equation) and to specify any global "later time" boundary conditions violates causality in a manner that must be considered unacceptable; information cannot logically propagate back from the future into the past. This, of course is consistent with the result[18] that a Fourier mode introduced into the solution of a time-dependent system of conservation laws possessing eigenvalues of nonzero imaginary part will grow exponentially. Nor is it possible to retrieve the situation simply by adding viscosity, for it can be shown[14] that for small values of viscosity there always exist disturbances that exhibit exponential growth rate, thus tainting the inviscid limit of the system. Quite apart from this, it is surely not unreasonable to expect that any viscous system should possess a consistent inviscid limit.

2. General equations for gas/particulate two-phase flow and their interpretation in one space dimension

Bearing in mind the discussion of the previous section and the general philosophy that we wish to adopt for the formulation of the equations of motion, we begin modelling from a rather general viewpoint. This ap-

proach is carefully outlined in Drew and Wood.[14] We assume at the outset that we are interested in each phase *separately*, and that averaging will take place only after formulation of the general equations for each phase.

Assuming that each phase is objective, so that the stress S satisfies $S(QF) = QS(F)Q^T$ for all deformation tensors F, where Q is a proper orthogonal tensor, and also that each phase is hyperelastic, so that the dissipation of energy in every part is non-negative for every cyclic motion and there exists a strain energy density function Ψ such that

$$S(F) = \rho \frac{\partial \Psi}{\partial F} F^T$$

then it only remains to decide the nature of the phases under consideration In order to make progress, we will ignore non-Newtonian effects. Denoting any conserved quantity by Σ, its velocity by q, its density by ρ, its molecular flux by J and assuming that the relevant source density is given by f, the conservation law for each phase can be written

$$\frac{\partial}{\partial t}(\rho\Sigma) + \nabla \cdot (\rho q\Sigma - J) = \rho f \qquad (1)$$

The generic equation of motion (1) is insufficient to fully determine the motion because the boundaries between the two phases are unknown; extra conditions are therefore required at the phase boundaries. These take the form of interfacial jump conditions[14] given by

$$f_i = [(\rho\Sigma(q - q_i) + J) \quad \hat{n}_i]_1^2$$

Here q_i represents interfacial velocity, f_i interfacial source density, and $\hat{n}_i$ the unit interface normal.

Our development of the equations of motion is very similar to that contained in Drew and Wood[14] (and other sources) and for this reason we omit nearly all of the details. After suitable choices have been made in (1), the equations of motion, written as conservation laws, and the jump conditions for each conserved quantity are given by

(Mass: $\Sigma = 1, J = 0, f = f_m, f_i = f_{mi}$)

$$\rho_t + \nabla \cdot (\rho q) = \rho f_m, \quad f_{mi} = [\rho(q - q_i) \cdot \hat{n}_i]_1^2$$

(Momentum: $\Sigma = q, J = T, f = f_p, f_i = f_{pi}$)

$$(\rho q)_t + \nabla \cdot \rho qq = \nabla \cdot T + \rho f_p,$$
$$f_{pi} = [(\rho q(q - q_i)) \cdot \hat{n}_i]_1^2$$

(Energy: $\Sigma = E, J = T \cdot q - \zeta, f = f_p \cdot q + r, f_i = \kappa_i$)

$$(\rho E)_t + \nabla \quad \rho Eq = \nabla \cdot (T \cdot q - \zeta) + \rho f_p \cdot q + \rho r$$
$$\kappa_i = [(\rho E(q - q_i) + T \cdot q - \zeta) \cdot \hat{n}_i]_1^2$$

Here the source terms for mass and momentum are given by f_m and f_p respectively (with a subscript i added for the interfacial terms), T is the stress tensor; E is the total energy, which is the sum of the internal energy e and $q^2/2$; ζ is the heat flux term; r is the heating source; and κ_i represents the sum of the interface heating source per unit area and the interface surface energy.

Accepting now that ensemble averaging must be used to circumvent the difficulty of the unmanageable amount of interface tracking that would result if we were to use the above equations for both phases separately, we use the three-dimensional ensemble averaging operator[11]

$$\bar{f}(x, t) = \frac{1}{\Delta t} \int_t^{t+\Delta t} f(x, \tau)\, d\tau$$

Introducing a phase indicator function χ_k which takes the value 1 when x is in phase k and zero otherwise, we average (1) using the fact that

$$\overline{\chi_k \nabla f} = \overline{\nabla \chi_k f} - \overline{f \nabla \chi_k}$$

and therefore

$$\overline{\chi_k \nabla f} = \nabla \overline{\chi_k f} - \overline{f \nabla \chi_k}$$

since *within each phase* the average of the derivative will be equal to the derivative of the average. It is the second term on the right-hand side of this equation that will give rise to contributions from the interfacial terms that will prove to be so important in the modelling. It is also easy to show that

$$(\chi_k)_t + q_i \cdot \nabla \chi_k = 0$$

and probably the easiest way to proceed is to multiply both sides of the general conservation laws by the indicator function and then average the result.

The ensemble-averaged system of equations ($k = 1$, 2) is (see Nomenclature list)

$$(\bar{\alpha}_k \bar{\rho}_k)_t + \nabla \cdot (\bar{\alpha}_k \bar{\rho}_k \bar{q}_k) = \bar{\Gamma}_k + \bar{f}_{mk} \qquad (2)$$

$$(\bar{\alpha}_k \bar{\rho}_k \bar{q}_k)_t + \nabla \quad (\bar{\alpha}_k \bar{\rho}_k \bar{q}_k)\bar{q}_k =$$
$$\nabla \cdot \bar{\alpha}_k \bar{T}_k + \bar{\alpha}_k \bar{\rho}_k \bar{f}_{pk} + \bar{M}_k + \bar{q}_{ki} \bar{\Gamma}_k \qquad (3)$$

$$(\bar{\alpha}_k \bar{\rho}_k (\bar{e}_k + \bar{q}_k^2/2))_t + \nabla \quad (\bar{\alpha}_k \bar{\rho}_k \bar{q}_k (\bar{e}_k + \bar{q}_k^2/2)) =$$
$$\nabla \cdot (\bar{\alpha}_k (\bar{T}_k \cdot \bar{q}_k - \bar{\zeta}_k)) + \bar{\alpha}_k \bar{\rho}_k (\bar{r}_k + \bar{f}_{pk} \cdot \bar{q}_k)$$
$$+ \bar{G}_k + \bar{W}_k + \overline{\Gamma_k e_{ki}} + \overline{\Gamma_k q_{ki}^2/2} \qquad (4)$$

An averaged entropy inequality may also be computed, and the interfacial jump conditions emerge after a multiplication of the exact jump condition by the product of the interfacial normal and the gradient of the phase indicator function, followed by an average.

So far, there has been an implicit assumption that all flow is smooth. As the averaging process proceeds, however, we have to ask the usual questions about whether the flow is laminar or turbulent. If turbulent flow is present, the effects may be introduced into the model in the usual way by considering the steady and the fluctuating components of a quantity. For simplicity we prefer to group the turbulent terms together as "turbulent stresses." The general procedure is not complicated, and relies on the fact that, if we write $q = \bar{q}_k + q_k'$, etc., then we find that with suitable definitions

$$\overline{\chi_k \rho \Sigma q} = \bar{\alpha}_k \bar{\rho}_k \bar{\Sigma}_k \bar{q}_k - \bar{\alpha}_k \bar{J}_k^{Re}$$

The superscript Re identifies contributions from turbulent effects. Having defined turbulent averaged quan-

tities (see Nomenclature) we therefore redefine

$$\bar{T}_k = \bar{T}_k + \bar{T}_k^{Re}, \quad \bar{\zeta}_k = \bar{\zeta}_k + \bar{\zeta}_k^{Re}, \quad \bar{e}_k = \bar{e}_k + \bar{e}_k^{Re}$$

in (2)–(4). Mixture equations may also be proposed by adding the phasic balance equations and applying the jump conditions. Of course, whether we decide to use the three-dimensional model above or the mixture equations, there are still many state assumptions that must be made to complete the formulation. It is the content and the reasoning behind these assumptions that constitutes the challenging problem in two-phase flow theory; they must include a sufficient amount of modelling information to characterize the system and render it totally hyperbolic.

Further simplifications may be made by using quasi one-dimensional assumptions. Cross-sectional area averaging will then allow the equations to be simplified to a system of conservation laws in one space dimension. The essence of the quasi one-dimensional assumption is that the cross-sectional area of the channel that confines the flow varies slowly in comparison with the radius of the duct, in which case the effects of varying cross-sectional area may be included in a one-dimensional model. For any variable $\bar{f}$ that has already been ensemble averaged we define

$$\langle \bar{f}(x,t) \rangle = \frac{1}{A(x)} \int\int_{A(x)} \bar{f}(x,t)\, dA$$

where $A(x)$ represents the cross-sectional area of the channel at ordinate x. The key averaging properties that are needed are explained in detail in Fitt,[19] and amount to the fact that

$$\frac{\partial \langle \bar{f} \rangle}{\partial t} = \left\langle \frac{\partial \bar{f}}{\partial t} \right\rangle$$

$$\langle f \rangle_x = -\frac{A'}{A}\langle f \rangle + \frac{1}{A}\oint_C \tilde{N}_1 f\, ds + \langle f_x \rangle$$

$$\langle \nabla f \rangle = \frac{1}{A}\oint_C \frac{fn}{N}\, ds + \frac{1}{A}[A\langle f \rangle]_x \hat{e}_x$$

where C is the boundary of the cross-sectional area $A(x)$; $\hat{e}_x$, $\hat{e}_y$, and $\hat{e}_z$ are unit vectors in the coordinate directions with x measured axially down the one-dimensional channel; s measures arc length; and $N = \boldsymbol{n} \cdot \boldsymbol{n}_2$, $N_1 = \sqrt{(1 - N^2)}/N$. Here $\boldsymbol{n}$ is the true normal to the channel wall and $\boldsymbol{n}_2$ is the normal to the channel wall projected onto the (y, z) plane.

Carrying out the averaging and taking the scalar product of the momentum equation with the unit vector in the x-direction, we retrieve the following phasic equations of motion (see Nomenclature list for definitions):

$$(\alpha_k \rho_k)_t + \frac{1}{A}(A\alpha_k \rho_k u_k)_x = \Gamma_k + f_{mk} \tag{5}$$

$$(\alpha_k \rho_k u_k)_t + \frac{1}{A}(A\alpha_k \rho_k u_k^2 C_{uk})_x = \frac{1}{A}(A\alpha_k (T_k + T_k^{Re}))_x + M_k + \frac{4}{D}\alpha_{kw} T_{kw} + u_{ki}\Gamma_k + \alpha_k \rho_k f_{pk} \tag{6}$$

$$(\alpha_k \rho_k (e_k + e_k^{Re} + u_k^2/2))_t + \frac{1}{A}(A\alpha_k \rho_k u_k C_{ek}(e_k + e_k^{Re} + u_k^2/2))_x$$
$$= -\frac{\xi_h}{A}\alpha_{kw}\zeta_{kw} + \frac{1}{A}(A\alpha_k((T_k + T_k^{Re})u_k - \zeta_k - \zeta_k^{Re}))_x + G_k + W_k + \alpha_k \rho_k (r_k + u_k f_{pk}) + (e_{ki} + u_{ki}^2/2)\Gamma_k \tag{7}$$

Again, an area-averaged entropy inequality and area-averaged jump conditions could be written down if we so desired. Some comments are necessary concerning the definitions of the variables. Many authors previously have omitted the profile coefficients in the momentum and energy equations. The need for these parameters arises from the fact that when cross-sectional averaging is performed, the product of the averages is not equal to the average of the products. If it were, then both C_{uk} and C_{ek} would take the value unity. These coefficients can have an important effect on the hyperbolicity of the system. Also, it is worth noting that our definitions have come a long way from the original variable definitions. For example, in terms of original variables even a simple quantity like the axial velocity is given by

$$u_k = \langle (\bar{\chi}_k \overline{\rho\chi_k}/\bar{\alpha}_k)(\overline{\chi_k \rho q}/\bar{\alpha}_k \bar{\rho}_k) \rangle \cdot \boldsymbol{e}_x / \langle \bar{\chi}_k \overline{\rho\chi_k}/\bar{\alpha}_k \rangle$$

It is therefore important to remember the precise definitions of the variables when the real modelling work begins below

3. The modelling of gas/particulate two-phase flows

Until now everything we have considered has been known previously, and it is for this reason that many of the details were omitted. It does, however, constitute essential background to the modelling details that will be considered now. We now turn explicitly to (5)–(7)

and consider how best to model the specific terms. We wish to reflect the exact nature of the flow under consideration; if we do not make the correct assumptions we cannot expect to recover a hyperbolic system In this study, attention is restricted to algebraic constitutive laws, although there are formulations that include derivatives and many other effects.[20]

We begin by making some assumptions (**A1–A11**): (in the descriptions below, some quantities are ignored as negligible. In order to be able to make such statements confidently, a full nondimensionalization and comparison of dimensionless groups is required. Although this is a simple task to carry out, the details are tedious and cumbersome and have been omitted).

A1. First we assume that $A(x)$ = constant, so that flow takes place in a pipe of constant cross-sectional area with axial direction x. The cross-sectional area is assumed to satisfy $L/A\ \partial A/\partial x \ll 1$ so that cross-sectional area averaging is valid.

A2. As far as the bulk source terms are concerned, we shall assume that $f_{mk} = r_k = 0$ and $f_{pk} = -g\hat{k}$ where $\hat{k}$ is a unit vector vertically downward and g is the acceleration due to gravity. Some explanation of these assumptions is necessary. In the standard internal ballistic cycle, ignition of the propellant bed takes place starting from ambient conditions, and all of the mass, momentum, and heat sources arise from interfacial effects, viz. the gasification of the propellant The only exception to this is in the very early stages of the cycle when (typically) hot primer gas is injected into the propellant to promote ignition. The mechanics of ignition will be ignored for simplicity, and it will be assumed that the propellant charge is ignited by a raised ambient temperature distribution within the charge. Gravity has been included because sometimes the gun tube is at an angle (especially for larger artillery pieces) such that $|\hat{k} \cdot \hat{e}_x| = \sin\theta$ is non-negligible. It is worth making the general point that although such source terms do not include derivatives of the dependent variables and so cannot influence the hyperbolicity of the system, it is nevertheless good practice to retain them in the equations; under some circumstances (which do not pertain here) there is a chance that to leading order they might dominate *all* of the derivative terms, thereby turning a partial differential equation into an algebraic relationship between the dependent variables.

A3. At present the parameters α_{kw}, T_{kw}, ζ_{kw}, and ξ_k all appear in the equations of motion. They arise naturally from the cross-sectional averaging of gradient quantities. We have already assumed that $q_k = 0$ at the walls to rid ourselves of some of these terms, and we shall also assume that $T_{kw} = \zeta_{kw} = 0$ so that there is no wall stress and no heat loss. Bearing in mind the fact that it is known[21] that these effects contribute only a few percent to the overall energy balance inside the chamber, it seems reasonable to dispose of them now and simplify the model.

A4. Next we consider the interfacial source terms. Γ_k represents the contribution to the kth mass balance equation from the gasification of the surfaces of the solid particles as they burn. For simplicity we assume Piobert's law whereby all burning surfaces recede at the same rate (burning by parallel layers). In this case, there is good experimental evidence[22] that

$$\Gamma_k \simeq (-1)^{k+1}\dot{m}$$

where

$$\dot{m} = \frac{m_0 N_2 h(\lambda)(b_1 + b_2 p_1^{\beta})}{A(x)}$$

Here m_0 represents the original mass of solids, p_1 the gas pressure, $h(\lambda)$ is an order unity nondimensional function of the propellant form function, which relates the fraction of burning surface remaining to the fraction of the charge mass burnt, b_1 and b_2 are known as the burning rate constant and the burning rate coefficient, respectively, and β is the pressure index, found experimentally to be close to unity N_2 is the number of solid particles per unit area, and in practice the easiest way to keep track of this quantity is to write down a separate conservation law of the form

$$N_{2t} + (u_2 N_2)_x = 0$$

Because this equation separates out from the rest of the system and has no effect on the hyperbolicity of the system, we shall assume that N_2 is given. Some modelling is also required to determine the interfacial velocity associated with the interfacial mass source term. For solid particles, it is usual to write

$$u_{ki} = u_2 \quad (k = 1, 2)$$

though if the flow is not highly dispersed this may not be very accurate. Similar reasoning leads to the approximation

$$e_{ki} = e_2$$

A5. Clearly there will be mass and momentum conservation laws for both phases, but the status of the energy balance law for the solid phase requires some examination. Because the solid phase is assumed to be composed of incompressible particles, we assume that an energy balance equation is required only for the gas phase This point of view has been contested in the past by Krier et al.[23] and Hoffman and Krier,[24] who proposed mixture equations using ad hoc arguments. However, their equations suffer from the defect that they have no steady state solution in which the void fraction is a nontrivial function of x.

A6. Next, we must determine the stress tensors and interfacial source terms in the momentum equations. We recall that by definition

$$\bar{M}_k = \overline{-T \cdot \nabla\chi_k}, \quad \bar{T}_k = \overline{\chi_k T}/\bar{\alpha}_k$$

the first term arising because of the interfacial terms introduced by the averaging. Assuming phase k to be a viscous compressible gas, we find that

$$T = -pI + 2\mu\tau;$$

$$(\tau)_{ij} = \tau_{ij} = \frac{1}{2}\left(\frac{\partial q_i}{\partial x_j} + \frac{\partial q_j}{\partial x_i}\right) - \frac{1}{3}\delta_{ij}\frac{\partial q_k}{\partial x_k}$$

From the definitions we see that

$$\bar{M}_k = \overline{p\boldsymbol{I}\cdot\nabla\chi_k} - \overline{2\mu\boldsymbol{\tau}\cdot\nabla\chi_k}$$

and at this stage it is normal to separate the interfacial pressure and shear stress out from the local interfacial effects by writing

$$\bar{M}_k = \bar{p}_{ki}\overline{\nabla\chi_k} - 2\mu\bar{\boldsymbol{\tau}}_{ki}\cdot\overline{\nabla\chi_k} + \bar{M}'_k = \bar{p}_{ki}\nabla\bar{\alpha}_k - 2\mu\bar{\boldsymbol{\tau}}_{ki}\nabla\bar{\alpha}_k + M'_k$$

where the term $\bar{M}'_k$ represents the added interfacial forces. Cross-sectional averaging then yields

$$M_k = \langle\bar{M}_k\rangle\cdot\boldsymbol{e}_x = \langle\bar{p}_{ki}\nabla\bar{\alpha}_k\rangle\cdot\boldsymbol{e}_x - \langle 2\mu\bar{\boldsymbol{\tau}}_{ki}\nabla\bar{\alpha}_k\rangle\cdot\boldsymbol{e}_x + M'_k$$

where $M'_k = \langle\bar{M}'_k\rangle\cdot\boldsymbol{e}_x$, and the traditional next step[11] is to assume that

$$\langle\bar{p}_{ki}\nabla\bar{\alpha}_k\rangle = p_{ki}\langle\nabla\bar{\alpha}_k\rangle$$

reflecting the fact that the averaged pressures do not change very much over a cross-section of the flow. As far as the interfacial shear stress is concerned, probably the best we can do is to introduce a profile parameter C_{ss}, a function of the void fraction, and write

$$\langle 2\mu\bar{\boldsymbol{\tau}}_{ki}\nabla\bar{\alpha}_k\rangle\cdot\boldsymbol{e}_x = 2\mu C_{ss}(\alpha)\tau_{kw}/D$$

where τ_{kw} is the wall shear stress, so that for a constant cross-sectional area

$$M_k = p_{ki}\frac{\partial\alpha_k}{\partial x} - 2\mu C_{ss}(\alpha)\tau_{kw}/D + M'_k$$

To calculate $\bar{\boldsymbol{T}}_k$, we note that

$$\bar{\boldsymbol{T}}_k = \overline{\chi_k(-p\boldsymbol{I})}/\bar{\alpha}_k + \overline{2\mu\boldsymbol{\tau}\chi_k}/\bar{\alpha}_k = -\bar{p}_k + \overline{(\mu(\nabla\boldsymbol{q}+\nabla\boldsymbol{q}^T) - 2\mu(\nabla\cdot\boldsymbol{q})\boldsymbol{I}/3)\chi_k}/\bar{\alpha}_k$$

The shear stress can be averaged[14] by introducing the kinematic viscosity $\nu = \mu/\rho$ and using the fact that

$$\overline{\chi_k\rho\nabla\boldsymbol{q}} = \bar{\alpha}_k\bar{\rho}_k\nabla\bar{\boldsymbol{q}}_k - \nabla(\bar{\alpha}_k\bar{\rho}_k)(\bar{\boldsymbol{q}}_{ki} - \bar{\boldsymbol{q}}_k)$$

so that averaging yields

$$\bar{\alpha}_k\bar{\boldsymbol{T}}_k = -\bar{\alpha}_k\bar{p}_k\boldsymbol{I} + 2\mu\bar{\alpha}_k\bar{\boldsymbol{\tau}}_k$$

where

$$2\mu\bar{\alpha}_k\bar{\boldsymbol{\tau}}_k = \nu_k[\bar{\alpha}_k\bar{\rho}_k(\nabla\bar{\boldsymbol{q}}_k + (\nabla\bar{\boldsymbol{q}}_k)^T) + (\bar{\boldsymbol{q}}_k - \bar{\boldsymbol{q}}_{ki})\nabla(\bar{\alpha}_k\bar{\rho}_k) + \nabla(\bar{\alpha}_k\bar{\rho}_k)(\bar{\boldsymbol{q}}_k - \bar{\boldsymbol{q}}_{ki}) - \tfrac{2}{3}[\bar{\alpha}_k\bar{\rho}_k(\nabla\bar{\boldsymbol{q}}_k) + \nabla(\bar{\alpha}_k\bar{\rho}_k)(\bar{\boldsymbol{q}}_k - \bar{\boldsymbol{q}}_{ki})]$$

Thence

$$\alpha_k T_k = -\alpha_k p_k + 2\mu\alpha_k\tau_k$$

where $\tau_k = \langle\bar{\boldsymbol{\tau}}_k\rangle\cdot\boldsymbol{e}_x\cdot\boldsymbol{e}_x/\bar{\alpha}_k$

For our purposes, the gas phase is phase 1, so that we have

$$M_1 = p_{1i}\frac{\partial\alpha_1}{\partial x} - 2\mu C_{ss}(\alpha)\tau_{1w}/D + M'_1,$$

$$\alpha_1 T_1 = -\alpha_1 p_1 + 2\mu\alpha_1\tau_1$$

The jump conditions give $M_1 = -M_2$, and assuming that phase 2 is dispersed in the form of distinct "blobs" within phase 1, the easiest assumption to make is that the stress tensor within phase 2 is given by

$$\boldsymbol{T}_2 = -p_2\boldsymbol{I}$$

where p_2 is constant for each particle, which is tantamount to assuming that the elastic forces acting on each particle are not sufficient to produce any elastic deformation.

We must also consider the roles played by interparticulate collisions and intergranular (particle/particle) stresses in the solid particles that occur when they are close packed. Experience shows that a typical bed of granular propellant exists mainly in one of two states; either it is close-packed with slowly moving or stationary large-sized particles that are capable of propagating stress waves through the bed, or it is highly dispersed, consisting of fast-moving particles, which are small owing to the large amount of gasification that has taken place. We therefore discount the effects of interparticular collisions (the particles are either too small and dispersed or too slow-moving to exchange appreciable amounts of momentum or energy) but allow for the propagation of intergranular stress waves by including an "intergranular stress" σ_g so that

$$\boldsymbol{T}_2 = -(p_2 + \sigma_g)\boldsymbol{I}$$

where

$$\sigma_g = \rho_1 c_1^2\alpha_0^2\left(\frac{1}{\alpha_1} - \frac{1}{\alpha_0}\right) \quad (\alpha_1 \le \alpha_0)$$

and is zero otherwise. In this simple model, the intergranular stress assumes importance when the bed is packed closely enough so that the gas volume fraction is less than some given "settling porosity" α_0 (normally taken to have a value of the order of 4/10) In such cases, stress is transmitted by intergranular stress waves propagating at an intergranular wave speed c_1, which we assume to be constant and known. (There are more complete formulations;[25] these involve the specification of a partial differential equation for σ_g). With these assumptions, the solid stress tensor finally becomes

$$\alpha_2 T_2 = -\alpha_2(p_2 + \sigma_g)$$

At this point, we will also neglect the gas viscosity; if the problem to be solved involved single-phase flow in a pipe then the natural choice of model would be an inviscid core flow, coupled to a boundary layer calculation at the pipe walls There is no reason to proceed in a different fashion here, and a nondimensionalization would show instantly that the gas viscosity may be ignored away from the pipe walls.

A7. As far as the pressures are concerned, we assume that p_1 is related to p_{1i} via some inviscid flow calculation. In general however, these two pressures will not be the same. Because the solid particles are incompressible, we have $p_{2i} \simeq p_2$ and because the solid needs no surface tension to support its boundary $p_{2i} = p_{1i}$ To complete the specification of the pressures

therefore we only need to relate p_1 and p_{1i}. For inviscid flow with velocity U_∞ past a sphere of radius a the pressure on the surface of the sphere has the form[26]

$$p|_{r=a} = p_\infty - \tfrac{1}{2}\rho_\infty U_\infty^2 F(\theta_s)$$

where p_∞ and ρ_∞ are the pressure and density, respectively, far away from the sphere and θ_s is the azimuthal angle. It thus seems very reasonable in our case to take

$$p_{1i} = p_1 - C_s\rho_1(u_1 - u_2)^2 \tag{8}$$

where C_s is an interfacial pressure coefficient that remains when the θ_s- dependence has been averaged out. For simple shapes, explicit values of C_s may be determined, but if the solid particles are irregular, then (8) would still seem to be the correct form to take for the interfacial pressure, though now all we know about the coefficient C_s is that to survive in the equations after nondimensional analysis has been carried out it must be $O(1)$.

A8. We must now consider the terms $\bar{M}_k'$. These correspond in general to all the forces that up to now have been omitted. Drew and Wood[14] list a number of components of this term including a viscous drag force, a virtual mass force, a lift force, a Faxen force and a Basset force. Thus

$$\bar{M}_1' = \boldsymbol{F}_D + \boldsymbol{F}_{vm} + \boldsymbol{F}_L + \boldsymbol{F}_{Fax} + \boldsymbol{F}_{Bas}$$

A careful nondimensionalization is needed here in general to decide which of these terms are important and which are not. In this particular regime the conclusions are fairly obvious. The lift force acts almost entirely out of the axial direction, and for solid "blobs" will be small anyway. The Faxen force is the additional contribution to the drag that arises from the torque in Stokes flow,[27] whereas the Basset force is a "start-up" force. Both contain positive powers of the gas viscosity and are therefore neglected. This leaves only the drag and virtual mass terms. For the latter (representing the additional drag force from the relative acceleration of the phases), the relevant force component F_i for a solid body in a stationary fluid is[26]

$$F_i = -\rho_\infty V_0 C_{ij}\dot{U}_{\infty j}$$

where V_0 is the volume of the solid body, $U_{\infty j}$ is the jth component of the body's velocity, C_{ij} is the tensor coefficient of virtual inertia, and a dot denotes total differentiation with respect to time. Accordingly we use

$$\boldsymbol{e}_x \cdot \boldsymbol{F}_{vm} = C_{vm}\rho_1\alpha_2[u_{1t} + u_1u_{1x} - (u_{2t} + u_2u_{2x})] \tag{9}$$

where the α_2 term reflects the averaging process and C_{vm} is a coefficient to be specified, which in general will be a function of the void fraction. There are many alternative models for the form of the virtual mass term and there is some controversy as to whether (9) is correct; for example, Geurst[28] formulated a model for bubbly flow using variational principles that has a different form to (9).

The drag is assumed to have the form

$$\boldsymbol{e}_x \cdot \boldsymbol{F}_D = C_D\alpha_2\rho_1(u_1 - u_2)^2 \tag{10}$$

which may be derived from dimensional arguments. For irregular shapes little is known about the drag coefficient C_D, save for the fact that it is likely to be a function of α_2, but for the present discussion this is not a serious problem as (10) does not include any differentiated terms and so will not contribute to the hyperbolicity analysis of the system. Having specified $\bar{M}_1'$, the averaged jump conditions imply

$$\bar{M}_1' \cdot \boldsymbol{e}_x = -\bar{M}_2' \cdot \boldsymbol{e}_x$$

so that $M_1' = -M_2'$.

A9. It remains to make some assumptions concerning the energy equation. The interfacial work term W_1 can be dealt with by introducing the interfacial velocity.[14] It is then possible to write

$$W_1 = -p_{1i}\alpha_{1t} + \overline{p(\boldsymbol{q} - \boldsymbol{q}_i)\cdot\nabla\chi_i} + \overline{p_{1i}'\boldsymbol{q}_i\cdot\nabla\chi_1 - \boldsymbol{\tau}\cdot\boldsymbol{q}\cdot\nabla\chi_1}$$

The interpretation of some of these quantities is difficult, but neglecting viscosity again, assuming that the interfacial velocity is given by u_2, and also that the term $\overline{\langle p(\boldsymbol{q} - \boldsymbol{q}_i)\cdot\nabla\chi_k\rangle}$ is negligible, we find that

$$W_1 = -p_{1i}\alpha_{1t} + M_1'u_2$$

We must also consider the interfacial energy source and energy flux terms; evidently the former will be small compared with the energy source arising from the burning, so that we may take $G_1 = 0$. The axial energy flux term may be modelled by assuming that

$$\zeta_1 = \alpha_2(u_1 - u_2)^3 d_L$$

where d_L is a *laminar energy friction factor.*

A10. Inevitably the turbulence assumptions are some of the hardest to feel confident about and clearly more work is needed here. However, for definiteness we make specific assumptions.

Drew and Wood[14] cite a number of possible models for the turbulent contributions to the stress tensor, the simplest of which amounts to

$$T_1^{Re} = \phi_T\alpha_2\rho_1(u_1 - u_2)^2 \quad \text{and} \quad T_2^{Re} = \frac{\rho_2}{\rho_1}T_1^{Re}$$

so that the dispersed phase is assumed to follow the motion of the continuous phase closely. The quantity ϕ_T is assumed to be available from experimental results (see section 4.2). The turbulent energy flux can now be modelled by the standard Reynolds analogy. This assumes that there is complete analogy between the transport of momentum and the transport of heat. Although this is one of the oldest and simplest theories for turbulent heat transport, it has been used successfully for many years and is known to be acceptably accurate for core regions of flow. Although under some circumstances modifications are necessary to model the turbulent heat transport in wall regions, we do not consider these complications here and simply write

$$\zeta_1^{Re} = d_T\alpha_2\rho_1(u_1 - u_2)(T_1 - T_2) + k_D^{Re}\frac{\partial T_1}{\partial x}$$

where d_T is a *turbulent energy friction factor* and k_D^{Re} is

a *turbulent conductivity*. We also assume that $e_1^{Re} = 0$, and, because we have ignored viscosities, it is consistent to take $k_D^{Re} = 0$.

A11. Last of all, we must consider the profile coefficients. The practical difficulties of proposing a theoretical model or undertaking experimental measurements of these coefficients have meant in the past that virtually all authors have taken each coefficient to be unity. In spite of the difficulties of obtaining values for C_{u1}, C_{u2}, and C_{e1} we shall leave them as free parameters in the model so that their influence on the hyperbolicity can be examined.

Using the assumptions A1–A11, the conservation laws finally become

$$(\alpha_1\rho_1)_t + (\alpha_1\rho_1 u_1)_x = \dot{m}$$

$$(\alpha_2\rho_2)_t + (\alpha_2\rho_2 u_2)_x = -\dot{m}$$

$$(\alpha_1\rho_1 u_1)_t + (\alpha_1\rho_1 u_1^2 C_{u1})_x + \alpha_1 p_{1x} = -C_s\rho_1(u_1 - u_2)^2\alpha_{1x} + (\alpha_1\phi_T\alpha_2\rho_1(u_1 - u_2)^2)_x + C_{vm}\alpha_2\rho_1[(u_{1t} + u_1u_{1x}) - (u_{2t} + u_2u_{2x})] + \dot{m}u_2 + C_D\alpha_2\rho_1(u_1 - u_2)^2 - \alpha_1\rho_1 g\sin\theta$$

$$(\alpha_2\rho_2 u_2)_t + (\alpha_2\rho_2 u_2^2 C_{u2})_x + \alpha_2 p_{1x} = \alpha_2[C_s\rho_1(u_1 - u_2)^2]_x + (\alpha_2^2\rho_2\phi_T(u_1 - u_2)^2)_x - C_{vm}\alpha_2\rho_1[(u_{1t} + u_1u_{1x}) - (u_{2t} + u_2u_{2x})] - \left(\alpha_2\rho_1 c_1^2\alpha_0^2\left(\frac{1}{\alpha_1} - \frac{1}{\alpha_0}\right)\right)_x - \dot{m}u_2 - C_D\alpha_2\rho_1(u_1 - u_2)^2 - \alpha_2\rho_2 g\sin\theta$$

$$(\alpha_1\rho_1(e_1 + u_1^2/2))_t + (\alpha_1\rho_1 u_1 C_{e1}(e_1 + u_1^2/2))_x + (p_1u_1\alpha_1)_x + p_1\alpha_{1t} = C_s\rho_1(u_1 - u_2)^2\alpha_{1t} - (d_L\alpha_2(u_1 - u_2)^3)_x + (\alpha_1u_1\phi_T\alpha_2\rho_1(u_1 - u_2)^2)_x - d_T(\alpha_2\rho_1(u_1 - u_2)(e_1 - T_2))_x + u_2C_{vm}\alpha_2\rho_1[(u_{1t} + u_1u_{1x}) - (u_{2t} + u_2u_{2x})] + C_D\alpha_2\rho_1u_2(u_1 - u_2)^2 - \alpha_1u_1\rho_1 g\sin\theta + \dot{m}(e_2 + u_2^2/2)$$

where $\alpha_1 + \alpha_2 = 1$ and ρ_2 is a given constant. The system is closed by selecting the relevant constitutive equation for the gas. In this case the perfect gas law

$$e_1 = \frac{p_1}{\rho_1(\gamma - 1)}$$

has been used, where γ is the usual ratio of specific heats, which we regard as being given; other constitutive equations may be used, but complicate the analysis.

This set of equations will be referred to henceforth as the working model.

4. Hyperbolicity analysis of the equations

The hyperbolicity of the working model can now be analyzed. It should be emphasized that in order to accomplish this task in any reasonable length of time, a symbolic manipulation package (MAPLE was used in the calculations reported below) is essential. Indeed, it is fair to say that before the advent of such algebraic computation systems, the calculations below would have been virtually impossible to perform.

The task is simply stated, but in practice the symbolic calculations required are large. The free parameters in the model are the profile coefficients C_{u1}, C_{u2}, and C_{e1} and the modelling parameters are ϕ_T, C_s, C_{vm}, c_1, d_L, and d_T, numbering nine in all.

The complexity of the system renders it unrealistic to expect to be able to perform a complete analysis, and we make no pretense of doing so. Rather the objective is to try to get a feeling for how the individual terms contribute to the analysis, and the nature of the qualitative changes in the hyperbolicity of the system that they may expedite. For a specific study, much more reliance would have to be placed on relevant experimental results and correlations for the submodels.

Writing the working model in the form

$$\boldsymbol{w}_t + A\boldsymbol{w}_x = \boldsymbol{b}$$

where A is a 5×5 matrix and $\boldsymbol{w}$ is the vector of unknowns $(\alpha_1, \rho_1, e_1, u_1, u_2)^T$, the eigenvalues λ_i are determined by solving the quintic equation $\det(A - \lambda_i I) = 0$. This was performed using a custom-written package[29] that greatly reduces the amount of tedious labor involved.

4.1. Determinant of the complete system

Performing the operations described above, the determinant of the conservation laws is found to be a quintic equation, containing 4759 terms, that does not factorize. However, it is illuminating to consider various special cases. The simplest of these is obtained by setting $C_{u1} = C_{u2} = C_{e1} = 1$ and $\phi_T = C_s = C_{vm} = c_1 = d_L = d_T = 0$, so that all of the added terms are ignored. The resulting system of equations has been used many times to study two-phase flow, and may be thought of as the "traditional" two-phase model. The determinant simplifies considerably in this case, giving eigenvalues $\lambda = u_1$ and $\lambda = yc + u_1$ where $c^2 = e_1\gamma(\gamma - 1)$ is the square of the gas sound speed and y satisfies the quartic equation

$$y^4 - 2Vy^3 + y^2(V^2 - 1 - q) + 2Vy - V^2 = 0 \quad (11)$$

where $V = (u_2 - u_1)/c$ and $q = \alpha_2\rho_1/\alpha_1\rho_2$. According to standard theory[30] the discriminant Δ of the quartic

$$ax^4 + bx^3 + cx^2 + dx + e = 0$$

is given by

$$\Delta = I^3 - 27J^2$$

where

$$I = ae - \frac{bd}{4} + \frac{c^2}{12},$$

$$J = \frac{ace}{6} + \frac{bcd}{48} - \frac{ad^2}{16} - \frac{c^3}{216} - \frac{eb^2}{16}$$

The equation possesses two real and two imaginary roots if $\Delta < 0$, and either four real or four imaginary roots if $\Delta > 0$. With reference to (11), we find that

$$\Delta = \frac{V^2 q}{16}(-27qV^2 - (q + 1 - V^2)^3)$$

so that

$$\Delta = -(1 - V^2 + q + 3q^{1/3} + 3q^{2/3})g(V^2, q)$$

where $g \geq 0$. Because (11) clearly possesses at least two real roots, the condition for four real roots when $q > 0$, $V^2 > 0$ is

$$V^2 > (1 + q^{1/3})^3 \tag{12}$$

The cases $V = 0$ and $q = 0$ must be dealt with separately; for $q = 0$ (no solid particles) we find that (11) has solutions $y = V, V, \pm 1$, whereas for $V = 0$, (11) has roots $0, 0, \pm\sqrt{1 + q}$ so that in both cases all four roots are real. These limits are singular ones, however; regular perturbation expansions show that for small q, (11) has roots

$$y = 1 + \frac{q}{2 - 4V + 2V^2} + O(q^2),$$

$$-1 + \frac{q}{-2 - 4V - 2V^2} + O(q^2)$$

and

$$V \pm \frac{qV}{\sqrt{V^2 - 1}} + O(q^2)$$

so that for any value of q greater than zero (12) applies, whereas for small values of V, (11) has roots

$$y = \pm\sqrt{1 + q} + \frac{qV}{1 + q} + O(V^2)$$

and

$$\frac{V(1 \pm \sqrt{-q})}{1 + q} + O(V^2)$$

so that for small V two of the roots are complex for any $q > 0$. This suggests that the worst case, as far as hyperbolicity is concerned, occurs in the neighborhood of $V = 0$, a fact that will be exploited below.

4.2. Analysis of the individual effects of the added terms

We now turn to an analysis of the individual effects of each of the added terms. Evidently the free parameters in the model may combine in complicated ways to affect the hyperbolicity of the model, but it is at least possible to acquire a feeling for how they each affect the eigenvalues by considering them one by one.

Fluctuation term. First we consider the individual effect of including only the fluctuation term. We find that the eigenvalues are given by $\lambda = u_1$ and $\lambda = yc + u_1$ where y satisfies

$$y^4 - 2Vy^3 + y^2(V^2 - 1 - q + (4 + \lambda)\Phi) + y\left(2V + \frac{2\Phi}{\alpha_1 V}(\Phi\alpha_1(R - 1)(1 - \gamma) - \alpha_1 V^2(1 + \gamma) + R - 1)\right) + \left(-V^2 - \frac{\Phi}{\alpha_1}(R - \alpha_1\gamma V^2 + \alpha_1 R\Phi(1 - \gamma))\right) = 0$$

Here R is the density ratio ρ_1/ρ_2 and $\Phi = V^2\alpha_2\phi_T$. The discriminant of this expression contains 2583 terms and so any inequalities such as (12) are rather difficult to obtain. Analysis may be performed for small V, however, and this gives the condition for real roots as

$$-16(\alpha_1 - 1)(\alpha_1 R - \alpha_1 - R)^3(-\alpha_1 R^2\phi_T + R^2\alpha_1\phi_T^2 + \alpha_1 R - \alpha_1 R\phi_T - 2\alpha_1 R\phi_T^2 + 2\alpha_1\phi_T + \alpha_1\phi_T^2 + R^2\phi_T - R^2\phi_T^2 + 2R\phi_T^2 - \phi_T^2) > 0$$

For hyperbolicity we therefore require

$$\alpha_1 < \frac{Q}{Q + R - R\phi_T + 2\phi_T}$$

where

$$Q = -R^2\phi_T + R^2\phi_T^2 - 2R\phi_T^2 + \phi_T^2$$

This condition sets an upper limit on α_1 for hyperbolicity that depends on the value of ϕ_T. An idea of the effect of the fluctuation terms can be obtained by using a particular value for ϕ_T. The values $-\frac{1}{3}$ and $-\frac{1}{5}$ have variously been cited[14,31] for ϕ_T so it seems reasonable to take $\phi_T = -\frac{1}{4}$. In this case we find that for hyperbolicity we require

$$\alpha_1 < \frac{5R^2 - 2R + 1}{5R^2 + 18R - 7}$$

so that for $R < -9/5 + 2\sqrt{29}/5 \sim 0.354$ the equations are never hyperbolic. For density ratios greater than this value but less than 0.4, we have hyperbolicity for any α_1, but the allowable range of α_1 decreases as R increases, until for $R = 1$ we must have $\alpha_1 < \frac{1}{4}$.

For the gas/particulate flows under consideration, we expect R to be quite small, so that although the fluctuation terms are certainly beneficial as far as hyperbolicity is concerned, the effect is not very important in this particular case.

Interfacial pressure term. We now consider the effect of the inclusion only of the interfacial pressure term. Now the eigenvalues are given by $\lambda = u_1$ and $\lambda = yc + u_1$ where y satisfies

$$y^4 + 2V(RC_s - 1)y^3 + y^2\left(\frac{RC_s\gamma V^2}{\alpha_1} - RC_s\gamma V^2 - 2RC_sV^2 + V^2 - 1 + R - \frac{R}{\alpha_1}\right)$$
$$+ 2Vy\left(1 - RC_s^2\gamma V^2 - \frac{RC_s}{\alpha_1} + \frac{RC_s^2\gamma V^2}{\alpha_1}\right) + V^2\left(-1 + RC_s - \frac{RC_s^2\gamma V^2}{\alpha_1} + \frac{RC_s}{\alpha_1} + RC_s^2\gamma V^2\right) = 0$$

The discriminant of the quartic is a quintic equation in V^2 that has 841 terms and suggests no obvious simplification. For small V, however, we can analyze the hyperbolicity by considering the coefficient of V^0 in the discriminant. This can be written as

$$\Delta = (\alpha_1 R - \alpha_1 - R)^3(\alpha_1^2 RC_s - \alpha_1^2 C_s - \alpha_1^2 + \alpha_1 C_s + \alpha_1 - RC_s - RC_s^2)$$

For the gas/particulate flows that form the focus of the current study we have $R < 1$, so that the condition for hyperbolicity for small V is

$$\alpha_1^2(-RC_s + C_s + 1) + \alpha_1(-1 - C_s) + RC_s(1 + C_s) > 0$$

The discriminant D of this is given by

$$D = (1 + C_s)(4R^2C_s^2 - 4RC_s^2 + C_s + 1 - 4RC_s)$$

so that when $0 < R < 1$ and $-1 < C_s < 0$ D is always positive. The region of hyperbolicity has therefore been extended to include the region

$$\frac{1 + C_s + \sqrt{D}}{2(1 + C_s - RC_s)} \leq \alpha_1 \leq 1$$

indicating that for small values of V the effect of the inclusion of the interfacial pressure terms is beneficial.

For large V, it has been shown that the equations with no added terms are always hyperbolic. An examination of the term multiplying the highest power of V in the discriminant indicates that for small α_2, hyperbolicity is preserved if

$$C_s < \frac{1}{2R}$$

a condition that will clearly pertain to a gas/particulate mixture and $O(1)$ interfacial pressure coefficients. We conclude that the inclusion of interfacial pressure forces is, in general, beneficial to the hyperbolicity of the equations.

Virtual mass term. To analyze the virtual mass term, the profile coefficients are given the value one and the other added terms are set as zero. The eigenvalues are once again given by $\lambda = u_1$ and $\lambda = yc + u_1$ where y satisfies the quartic equation

$$y^4(1 + TC_{vm}) + y^3(-2V - VC_{vm}(T\alpha_1(3 - \gamma) + R(1 - \gamma))/\alpha_1) + y^2(V^2 - q - 1 + C_{vm}(R(1/\alpha_1 + 2V^2(1 - \gamma))/\alpha_1) + (3 - 2\gamma)V^2T) + y(2V + C_{vm}V^3(-T(1 - \gamma) + R(\gamma - 1 - 2/V^2)/\alpha_1)) + V^2(-1 + RC_{vm}/\alpha_1) = 0$$

where $T = 1 - R - 1/\alpha_1$. The discriminant of this quartic has 2556 terms, but an analysis can be performed for the cases of both small and large V. For large V, either

$$\alpha_1 > C_{vm}, \quad \alpha_1 > \frac{C_{vm}(\gamma(1 - R) - R)}{1 + \gamma C_{vm}(1 - R)}$$

or

$$\alpha_1 < C_{vm}, \quad \alpha_1 < \frac{C_{vm}(\gamma(1 - R) - R)}{1 + \gamma C_{vm}(1 - R)}$$

ensure hyperbolicity For typical values of $R = \frac{1}{5}$, $C_{vm} = \frac{1}{2}$, and $\gamma = \frac{6}{5}$, the requirements amount to $\alpha_1 > \frac{1}{2}$ or $\alpha_1 < \frac{19}{74}$.

For small V, the conditions are slightly more complicated, but the final requirements are that $\alpha_1 < C_{vm}$ and

$$(C_{vm}\alpha_1(R - 1) + C_{vm} - \alpha_1)(\alpha_1 - RC_{vm})(\alpha_1^2(R - 1) + R(C_{vm} - \alpha_1)) > 0$$

A general condition for hyperbolicity is simple but tedious to obtain, but again using the typical values $R = \frac{1}{5}$ and $C_{vm} = \frac{1}{2}$ we find that the requirement for hyperbolicity is that either $\frac{1}{10} < \alpha_1 < \frac{1}{4}$ or $\frac{5}{14} < \alpha_1 < \frac{1}{2}$, showing that, as in bubbly flow, the virtual mass term can improve the hyperbolicity of the system for small V

Intergranular stress term. When the intergranular stress term alone is included, the eigenvalues are given by $\lambda = u_1$ and $\lambda = yc + u_1$ where y now satisfies the quartic equation

$$y^4 - 2Vy^3 + y^2\left(V^2 - 1 - q + q\mu^2\left(\frac{\alpha_1\alpha_0 + \alpha_1 - 2\alpha_0}{\alpha_0\alpha_1\alpha_2}\right)\right) + 2Vy - V^2 + q\mu^2\left(\frac{-\alpha_1^2 + \alpha_0}{\alpha_0\alpha_1\alpha_2}\right) = 0$$

with $\mu = c_1\alpha_0/c$. For small V the discriminant has the value

$$\frac{Rc_1^2}{64c^{10}\alpha_1^{10}}(\alpha_0 - \alpha_1^2)(g(\alpha_1, R, c, c_1))^2$$

where g is a quartic in α_1. The hyperbolicity condition is therefore $\alpha_1 < \sqrt{\alpha_0}$. Because the intergranular stress

law applies only for values of α_1 less than or equal to α_0, for small enough V the equations will always be hyperbolic if the law applies. For large values of V the discriminant of the quartic is

$$\frac{-16(-c^2\alpha_1\alpha_2 + \alpha_0 c_1^2(\alpha_1\alpha_0 + \alpha_1 - 2\alpha_0)}{c^2\alpha_1^2\rho_2}$$

so that in this limit the equations are hyperbolic for all values of c_1/c provided $\alpha_1 < 2\alpha_0/(1 + \alpha_0)$. Experiments suggest that a reasonable estimate for α_0 is about $\frac{4}{10}$ for many materials, and hyperbolicity thus pertains for $\alpha_1 < \frac{4}{7}$ for large V, and so in effect for all V whenever the stress law applies. The intergranular stress therefore has a markedly beneficial effect upon hyperbolicity. In most internal ballistics applications, however, the initially packed bed is soon dispersed as the solids gasify, so that the stress law may apply only for a small time during a typical flow.

Laminar energy friction factor term. When d_L alone is included in the equations, the eigenvalues are given by $\lambda = u_1$ and $\lambda = yc + u_1$. The quartic equation for y is

$$y^4 - 2Vy^3 + y^2\left(V^2 - q - 1 + \frac{3W(1-R)}{\rho_2 R}\right) + y\left(2V + \frac{2VW(R-3)}{\rho_2 R}\right) + V^2\left(-1 + \frac{3W}{\rho_1}\right) = 0$$

where $W = V^2 d_L \alpha_2(1 - \gamma)/\alpha_1$. For small V, the discriminant is

$$-\frac{16}{\alpha_1^4\rho_2^4}\rho_1\alpha_2(\rho_1\alpha_2 + \alpha_1\rho_2)^3$$

so that the inclusion of this term alters nothing and the equations are not hyperbolic.

For large V the discriminant is harder to analyze, but we can write

$$\Delta = -3\rho_2^4\rho_1^3\alpha_1^3 + d_L P_1(27\rho_2^2 + 30\rho_2\rho_1 - \rho_1^2) + P_2(-9\rho_2^3 + \rho_1^3 - 11\rho_2\rho_1^2 - 29\rho_2^2\rho_1) + d_L^3 P_3(\rho_2 - \rho_1)^3$$

where P_1, P_2, and P_3 represent terms that are always positive for $\gamma > 1$. For gas/particulate flow we always have $\rho_2 > \rho_1$, so Δ is negative for $d_L < 0$ and the equations are never hyperbolic for large V. For values of d_L greater than zero, it can be shown that, treated as a cubic in d_L, the discriminant δ of Δ can be written as

$$\delta = -27(\gamma - 1)^6\alpha_2^6(\rho_1 + 3\rho_2)^2(\rho_1^2 + 14\rho_1\rho_2 + 81\rho_2^2)^3\rho_2^6\rho_1^8\alpha_1^6$$

and so is always negative. Therefore the equation possesses three real and unequal roots. Denoting these (in increasing order) by d_{L1}, d_{L2} and d_{L3}, we conclude that for large V the equations are always hyperbolic when $0 < d_{L1} < d_L < d_{L2}$ or $d_{L3} < d_L$. In view of these restrictions, it seems that the inclusion of the laminar energy friction factor is not very helpful; however, it would be interesting to compare experimental results with the restrictions placed on d_L above.

Turbulent energy friction factor term. An analysis of the effect of the inclusion of the turbulent energy friction factor term d_T is rendered difficult by the uncertain nature of the coefficient—although we have assumed tacitly that it is order unity, it is not even clear whether it is positive or negative. References and experimental evidence are very hard to locate, and so all we can do is consider a general value of d_T. A further complicating fact is that, unlike most of the cases considered above, the resulting quintic equation does not factorize, so analysis of the discriminant is prohibitively long, even using symbolic algebra. A numerical investigation can be performed without too much trouble, however. Solving the relevant quintic equation using the NAG routine C02AEF, the regions of hyperbolicity can be plotted for various values of the parameters. *Figure 1* shows a hyperbolicity map for $\gamma = \frac{6}{5}$, $R = \frac{1}{5}$, $T_2/c^2 = 2$, and $d_T = \pm\frac{5}{7}$. V^2 is plotted against α_1 and solid lines divide parameter space into regions where the equations are totally hyperbolic (marked "H"), and those where complex eigenvalues exist. A further solid line (marked "L") is the curve $V^2 = (1 + q^{1/3})^3$, the hyperbolicity boundary for the equations with no added terms. We observe that for positive d_T the hyperbolicity region is increased in extent for $V > 1$, whereas for negative d_T the region splits into two distinct parts In neither case, however, is the region of hyperbolicity enhanced for $V < 1$. Some comments on the values of the parameters chosen are apposite. In general, the quintic depends on V, α_1, γ, R, T_2/c^2, and d_T, so that a full hyperbolicity analysis would require the consideration of six-dimensional parameter space. By choosing "reasonable" values for the parameters that remain nearly constant throughout the flow, however, we can reduce the dimension of the problem. The value of γ chosen above is typical for a highly reactive gas/particulate flow, whereas in reality the value of R normally varies from $R \sim 5 \times 10^{-4}$ (solid propellant of density ~1660 kg/m^3, gas at atmospheric conditions) to $R \sim \frac{1}{5}$ (gas at a temperature of ~3000 K, a pressure of ~350 MPa, and a density of ~330 kg/m^3). The value of d_T is chosen to be either positive or negative, but order one, whereas the value of T_2/c^2 is chosen simply to be order one. In fact, this final approximation is probably the most inaccurate. The solid temperature is determined by the adiabatic flame temperature,[21] which will be $O(10^3)$ while c^2 is usually in the range 10^5 to 10^6. In many cases therefore the parameter T_2/c^2 may be considered to be small, and this simplifies the analysis considerably. Ignoring terms of order T_2/c^2 we find that the resulting quintic equation factorizes, giving an eigenvalue $y = 0$ (in the usual notation) and the quartic equation

$$y^4 + y^3(-2V + Vd_T\alpha_2/\alpha_1) + y^2\left(V^2 - 1 - q + \frac{\alpha_2 d_T}{\alpha_1\gamma}(R - 1 - 2V^2\gamma)\right) + y\left(2V + \frac{\alpha_2}{\alpha_1\gamma}Vd_T(2 + V^2\gamma)\right) + \left(-V^2 - \frac{\alpha_2}{\alpha_1\gamma}d_T V^2\right) = 0$$

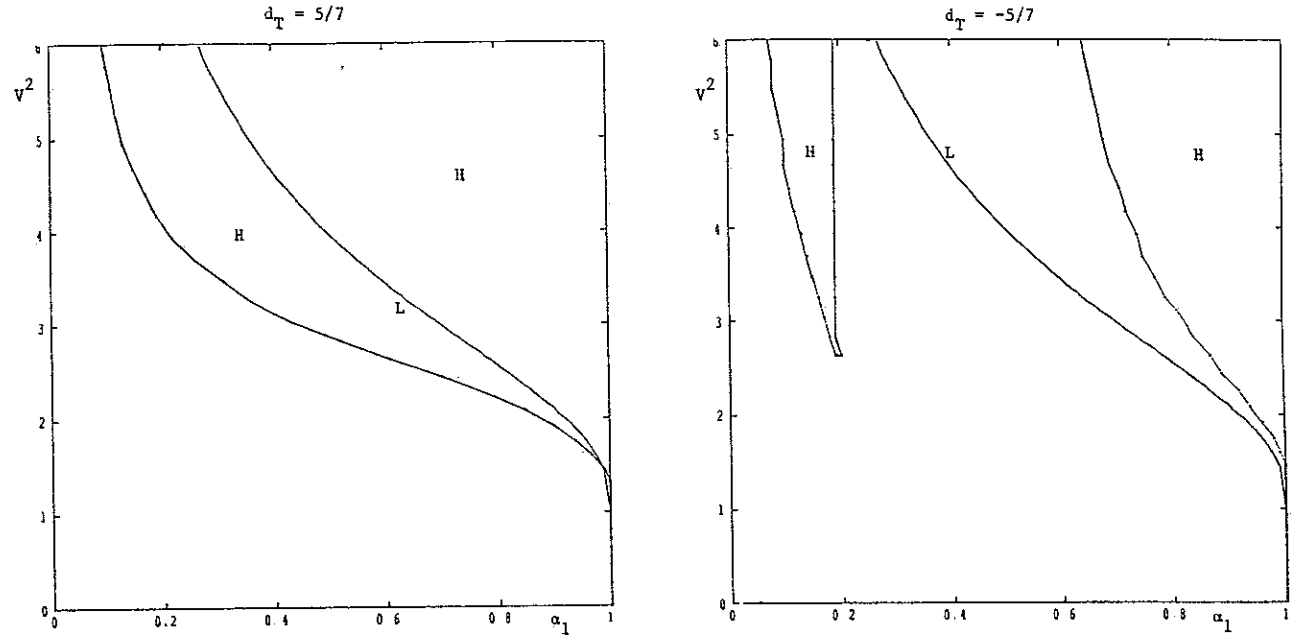

Figure 1 Hyperbolicity maps showing the influence of turbulent energy friction factor ($\gamma = \frac{6}{5}$, $R = \frac{1}{5}$, $T_2/c^2 = 2$)

Using the discriminant, an analysis can be performed for small V, showing that the condition for hyperbolicity is

$$\alpha_2(\gamma - d_T)(-\alpha_1\gamma - \alpha_2 d_T)((R\alpha_2 + \alpha_1)(\gamma - d_T) + d_T)^3 > 0$$

It is easy to show that for $d_T > \gamma$ the condition for hyperbolicity is always fulfilled, whereas there can never be hyperbolicity if $\gamma > d_T > 0$. For $d_T < 0$, the condition is

$$\frac{\alpha_1\gamma}{\alpha_2} < -d_T < \frac{\alpha_1\gamma}{\alpha_2} + \frac{\gamma R}{\alpha_2(1 - R)} \tag{13}$$

A large-V analysis is also possible; the hyperbolicity condition is

$$d_T^3(d_T - \gamma)(-\alpha_1 - \alpha_2 d_T)^3 > 0$$

thus the equations cannot be hyperbolic for $d_T > \gamma$, are always hyperbolic for $\gamma > d_T > 0$, and are hyperbolic for $d_T < 0$ provided $-d_T < \alpha_1/\alpha_2$. The large and small V analyses together indicate that negative values of d_T are probably more beneficial to the equations as far as hyperbolicity is concerned.

Figure 2 shows a numerical hyperbolicity map for the parameters $d_T = \pm\frac{5}{7}$, γ and R as in *Figure 1*, and $T_2/c^2 = 0.001$. The results of the small T_2/c^2 analysis are confirmed; for the values of the parameters taken, (13) implies that for the negative d_T case we have hyperbolicity if $0.216 < \alpha_1 < 0.373$, although the region concerned is very small.

Profile coefficients. The effect of the profile coefficients is somewhat harder to determine than in most of the cases considered above, as now u_1 is no longer an eigenvalue, giving a quintic characteristic equation. To give an idea of the kinds of results that can be obtained, we consider the case $C_{e1} = 1$, $C_{u2} = C_{u1}$. Setting $u_1 = cV_1$, $u_2 = cV_2$, $R = \rho_1/\rho_2$, and $\lambda = \gamma c$, we find that the resulting quintic depends on the parameters γ, V_1, V_2, R, α_1, and C_{u1}. Proceeding again by numerical means for given R, γ, and C_{u1}, we have specified V_2 and plotted hyperbolicity regions on a graph relating α_1 to $V^2(= (V_2 - V_1)^2)$. *Figure 3* shows the two cases $\gamma = \frac{6}{5}$, $R = \frac{1}{5}$, $V_2 = 0.1$, and $C_{u1} = 1.1$ and 1.5, respectively. The value of V_2 corresponds to a typical order of magnitude of solid velocity observed in highly reactive gas/particulate flows. As the profile coefficient increases, the hyperbolicity region becomes larger, and is extended to include points where both V and α_1 are small. The immediate conclusion from this limited study of profile coefficients is that they may have an important effect on the hyperbolicity of the equations. It is therefore unfortunate that there are such obvious practical difficulties in obtaining even the coarsest of estimates for these profile coefficients.

4.3 *More complicated combinations of terms*

As yet, we have only considered the effects of the added terms in isolation. Evidently, it is possible for them to combine with each other in complicated ways. We therefore further consider the character of the conservation laws for various combinations of the added terms. Unlike the case when all the added terms are zero, the hyperbolicity does not depend only on the quantities V and q, but in general on all of the flow variables, which are themselves unknown. The cases considered below can therefore give only an indication of the possible effects of the added terms.

Combined effect of intergranular stress and interfacial pressure. A particularly interesting combination of terms to consider is that involving the intergranular

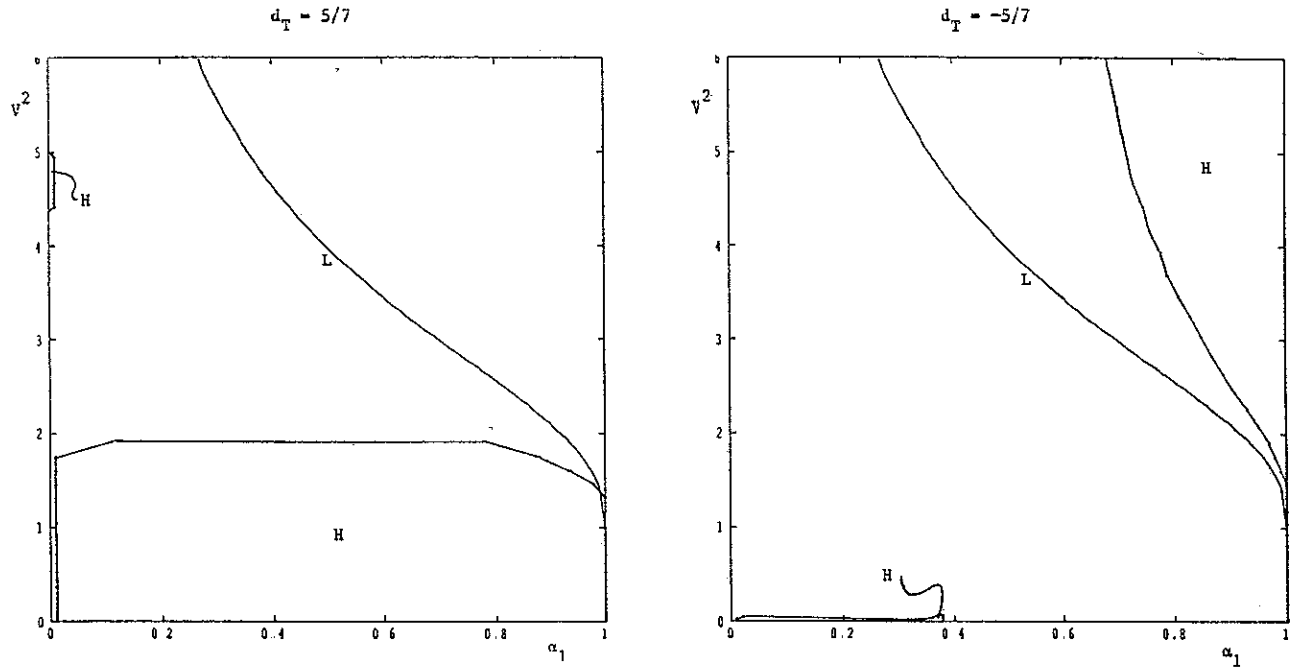

Figure 2 Hyperbolicity maps showing the influence of turbulent energy friction factor ($\gamma = \frac{6}{5}$, $R = \frac{1}{5}$, $T_2/c^2 = 0.001$)

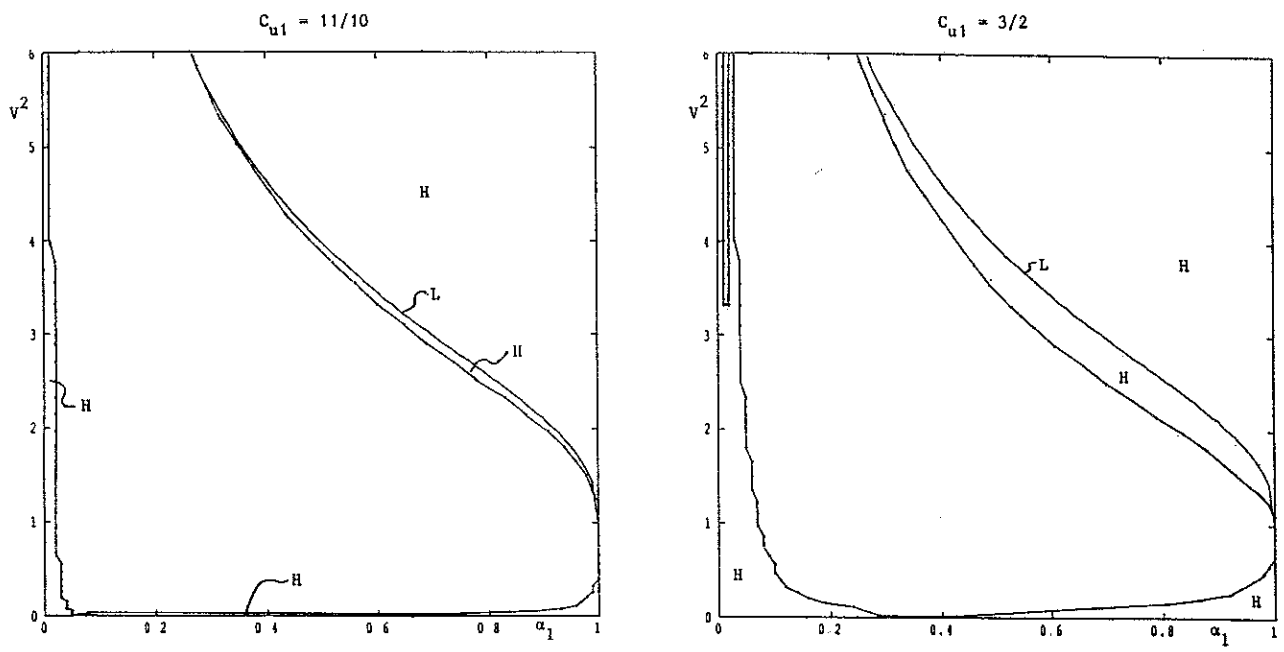

Figure 3 Hyperbolicity maps showing the influence of profile coefficients ($\gamma = \frac{6}{5}$, $R = \frac{1}{5}$, $V_2 = \frac{1}{10}$)

stress and the interfacial pressure, as both have been cited in the past as terms that may render the equations hyperbolic.[8,25] In this case one eigenvalue is given by $\lambda = u_1$, and the other four are determined by a quartic equation for y in the normal way. Fixing the quantities R, $C = c_1/c$, α_0, γ, and C_s once again allows us to plot V^2 against α_1 to determine the hyperbolic regions of phase space. *Figure 4* shows two such plots; in both cases we use $\gamma = \frac{6}{5}$, $\alpha_0 = 0.5$, and $C_s = -\frac{7}{16}$. In the first of the two figures we assume that the flow is well established and again we use the typical values $R = \rho_1/\rho_2 = \frac{1}{5}$ and $C = c_1/c = 1$. This value for C corresponds to an intergranular wave speed $c_1 = 1250$ m/sec (accurate measurements for this quantity have been made) and a pressure and density of 334.8 MPa and 300 kg/m^3, respectively, which are typical values for an internal ballistics application. The second figure relates to a much earlier part of the flow, and assumes that $\rho_1 = 75$ kg/m^3 and $p_1 = 43.4$ MPa. The hyperbolicity regions in both cases are quite different. The

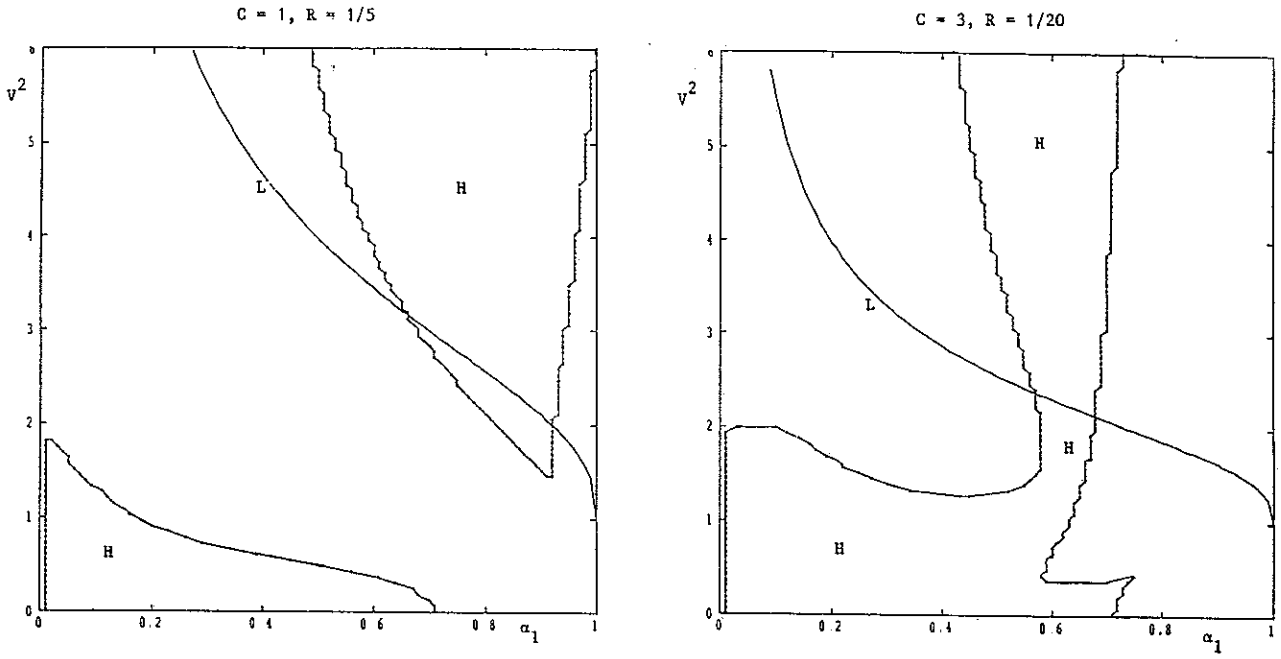

Figure 4. Hyperbolicity maps showing the combined influence of intergranular stress and interfacial pressure ($\gamma = \frac{6}{5}$, $\alpha_0 = \frac{1}{2}$, $C_s = -\frac{7}{16}$).

discriminant of the quartic contains 4299 terms and is a sixth-order polynomial in V^2. The parameter C_s does not appear in the zero coefficient of V term in the discriminant, however; thus for small V the hyperbolicity is independent of the interfacial pressure term, and the result of 4.2.4 applies. Both graphs confirm that for small V we simply require $\alpha_1 < 1/\sqrt{2}$ for hyperbolicity.

Finally, it is worth making the point that the graphs in *Figure 4* show clearly that, although the situation is certainly improved for small V by the addition of both interfacial pressure and intergranular stress terms, their addition by no means constitutes a universal panacea.

Combined effect of all the added terms. When all the added terms are included, the quintic equation that determines the eigenvalues is too unwieldy to permit a theoretical hyperbolicity analysis, and we must turn once again to purely numerical means. Evidently there are also a prohibitive number of cases that could be considered; for brevity only two examples are shown. Results were generated efficiently using the MAPLE facility for generating double precision optimized FORTRAN code. Such a facility is vital as the coefficients of the quintic eigenvalue equation typically contain on the order of 100 terms, rendering manual coding prone to errors.

The graphs in *Figure 5* show hyperbolicity maps with V plotted against α_1. In both figures the values $C_s = -\frac{7}{16}$, $C_{vm} = \frac{1}{2}$, $\gamma = \frac{6}{5}$, $\alpha_0 = \frac{1}{2}$, $\phi_T = -\frac{1}{4}$, $c_1 = 1250$, $d_L = \frac{1}{2}$, and $\rho_2 = 1500$ were used, while in the first graph the values used were $C_{u1} = C_{u2} = C_{e1} = \frac{11}{10}$, $d_T = \frac{1}{2}$, $\rho_1 = 100$, $T_2 = 2400$, $c = 1095$, and $u_2 = 10$ The second graph shows the case where $C_{u1} = C_{u2} = C_{e1} = \frac{12}{10}$, $d_T = -\frac{1}{2}$, $\rho_1 = 400$, $T_2 = 3200$, $p_1 = 300$, and $u_2 = 1000$. For values of V less than unity, there is a significant increase in the area of parameter space, which is hyperbolic in both cases, although for values of V greater than two the hyperbolicity region is actually decreased. Both figures provide a graphic illustration of the complexity of the manner in which the added terms combine to influence the hyperbolicity. It must be remembered, however, that to derive these results, we have been compelled to estimate not only the coefficients of the added terms, but also some of the dependent variables; there is no *a priori* reason why the differential equations should possess solutions that pass through this region of parameter space.

5. Summary and conclusions

A methodology has been explained whereby the character of the averaged equations of two-phase flow may be investigated. The model is based on a generalized theory for two-phase flow that has recently been developed and relies on the premise that the equations of motion can only model physical reality in an acceptable manner if terms that have effectively been removed by the process of ensemble averaging are replaced by suitable "added terms." Although these added terms greatly increase the complexity of the equations, if analysis shows that they may contribute to leading order, then they must be retained.

Theoretical and numerical analysis has been used to investigate the effect of these added terms on the hyperbolicity of the equations of motion, concentrating for illustrative purposes on a particular gas/particulate flow. The analysis shows that, though the added terms combine in a complicated manner, their individual effects can be quantified and understood, and, individu-

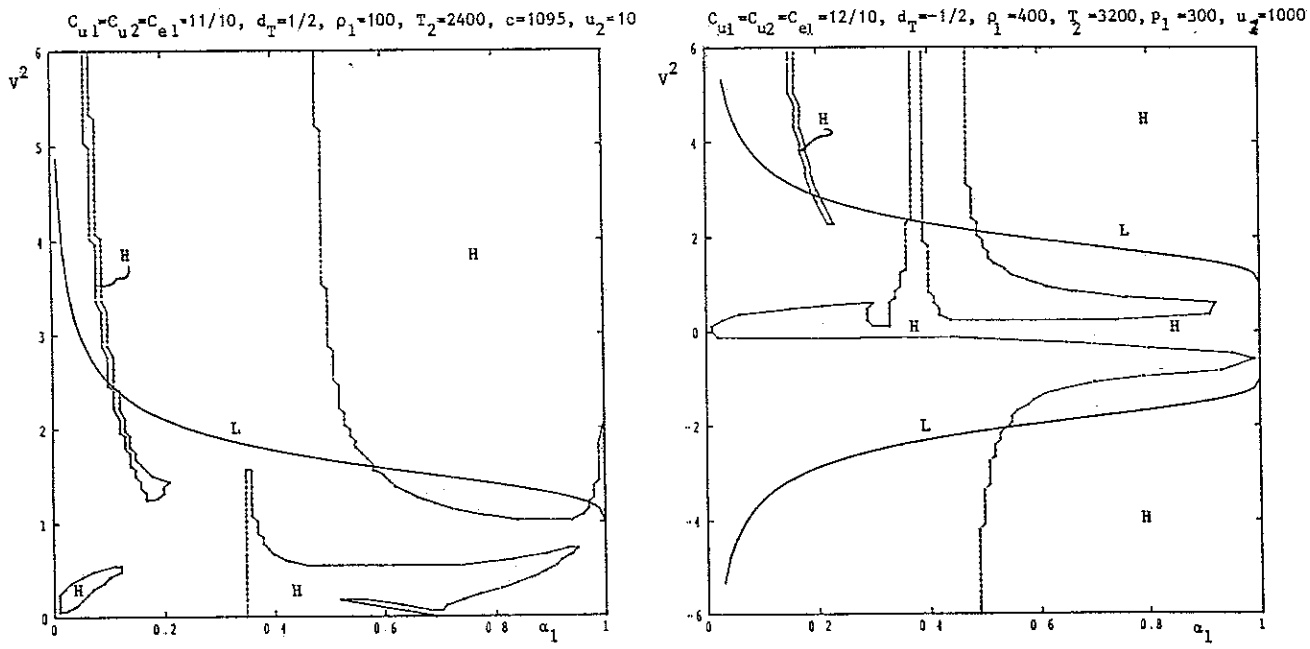

Figure 5. Hyperbolicity maps showing the influence of all added terms ($C_s = -\frac{7}{16}$, $C_{vm} = \frac{1}{2}$, $\gamma = \frac{6}{5}$, $\alpha_0 = \frac{1}{2}$, $\phi_T = -\frac{1}{4}$, $c_1 = 1250$, $d_L = \frac{1}{2}$, $\rho_2 = 1500$)

ally or in combined form, on occasions they may significantly improve the area of parameter space for which the equations are hyperbolic and may therefore be solved numerically with some success.

In general, for specific cases a careful nondimensional analysis of the equations is required to determine which of the added terms must be retained. When this has been carried out, the submodels appropriate to the particular regime(s) that pertain must be considered. Our ability to propose a rational and successful model for each different type of two-phase flow will depend on the sophistication and accuracy of these submodels. Most important, the analysis above suggests that it is simply unrealistic to propose a *single* simple "basic model" for all two-phase flows, and, merely by appending a selection of correlations, expect to recover a set of equations whose solutions mimic reality to an acceptable degree. The diversity and complexity of two-phase flow are simply too great.

Nomenclature

a	radius of sphere
α_0	settling porosity of solid phase
b_1	burning rate constant
b_2	burning rate coefficient
β	pressure index
c_1	intergranular wave speed
C	boundary of $A(x)$
C_{ij}	tensor coefficient of virtual inertia
E	total energy $= e + \frac{1}{2}q^2$
e	internal energy
$\hat{\boldsymbol{e}}_x$	unit vector pointing along tube axis
$\boldsymbol{F}$	deformation tensor
f	source density
f_i	interfacial source density
f_m	mass source term
f_{mi}	interfacial mass source term
f_p	momentum source term
f_{pi}	interfacial momentum source term
g	acceleration due to gravity
$h(\theta)$	function of propellant shape
$\boldsymbol{I}$	identity tensor
$\boldsymbol{J}$	molecular flux
k	1 (gas phase), 2 (solid phase)
k_D^{Re}	turbulent conductivity
$\hat{\boldsymbol{k}}$	unit vector vertically downward
κ_i	interface surface energy and heating source
L	typical pipe length
λ	propellant form function
m_0	original propellant charge mass
$\dot{m}$	interfacial mass source term
μ	gas viscosity
$\boldsymbol{n}$	normal to channel wall
$\hat{\boldsymbol{n}}_i$	unit interfacial normal
$\boldsymbol{n}_2$	projection of channel wall normal
N	$\boldsymbol{n}\ \boldsymbol{n}_2$
N_1	$\sqrt{1 - N^2}/N$
N_2	number of solid particles per unit area
$\nu = \mu/\rho$	gas kinematic viscosity
p	pressure
p_∞	pressure at infinity for flow past a sphere
Ψ	strain energy density
$\boldsymbol{Q}$	proper orthogonal tensor
$\boldsymbol{q}$	velocity
$\boldsymbol{q}_i$	interfacial velocity
r	heating source
U_∞	speed at infinity for flow past a sphere
V_0	volume of solid particle
ρ	density

ρ_∞ density at infinity for flow past a sphere
S stress tensor
σ_g intergranular stress (nominal loading)
Σ conserved quantity
t time
Δt time increment used in ensemble averaging
T stress tensor
τ viscous shear stress
θ angle of inclination of pipe to vertical
θ_s azimuthal angle for flow past a sphere
χ_k phase indicator function
x position vector
ζ heat flux

Ensemble-averaged quantities

$\bar{\alpha}_k$ $\overline{\chi_k}$ = volume fraction
$\bar{e}_k$ $\overline{\rho e \chi_k}/\overline{\rho_k \alpha_k}$ = internal energy
$\overline{e_{ki}\Gamma_k}$ $\overline{\rho e(q - q_i)\cdot\nabla\chi_k}$ = interfacial internal energy flux
$\bar{e}_k^{Re}$ $\overline{\frac{1}{2}\chi_k\rho_k q'^2_k}/\bar{\alpha}_k$ = turbulent kinetic energy
$\bar{f}_{mk}$ $\overline{\rho f_m \chi_k}/\bar{\rho}_k$ = bulk mass source
$\bar{f}_{pk}$ $\overline{\rho f_p \chi_k}/\bar{\alpha}_k\bar{\rho}_k$ = bulk momentum source
$\bar{G}_k$ $\overline{\zeta\cdot\nabla\chi_k}$ = interfacial heat source
$\bar{\Gamma}_k$ $\overline{\rho(q - q_i)\cdot\nabla\chi_k}$ = interfacial mass source
$\bar{M}_k$ $-\overline{T\cdot\nabla\chi_k}$ = interfacial momentum source
$\bar{M}'_k$ added interfacial forces
$\bar{p}_k$ $\overline{p\chi_k}/\bar{\alpha}_k$ = pressure
$\bar{p}_{ki}$ interfacial pressure
$\bar{q}_k$ $\overline{\chi_k\rho q}/\bar{\alpha}_k\bar{\rho}_k$ = velocity
q'_k turbulent fluctuation in q_k
$\overline{\frac{1}{2}q_{ki}^2\Gamma_k}$ $\overline{\frac{1}{2}\rho q^2(q - q_i)\cdot\nabla\chi_k}$ = interfacial kinetic energy flux
$\overline{q_{ki}\Gamma_k}$ $\overline{\rho q(q - q_i)\cdot\nabla\chi_k}$ = interfacial momentum flux
$\bar{r}_k$ $\overline{r\rho\chi_k}/\bar{\alpha}_k\bar{\rho}_k$ = heating source
$\bar{\rho}_k$ $\overline{\rho\chi_k}/\bar{\alpha}_k$ = density
$\bar{T}_k$ $\overline{\chi_k T}/\overline{\alpha_k}$ = stress tensor
$\bar{T}_k^{Re}$ $-\overline{\chi_k\rho_k q'_k q'_k}/\bar{\alpha}_k$ = Reynolds stress
$\bar{\tau}_k$ shear stress
$\bar{\tau}_{ki}$ interfacial shear stress
$\bar{W}_k$ $-\overline{(T\cdot q)\cdot\nabla\chi_k}$ = interfacial work
$\bar{\zeta}_k$ $\overline{\zeta\chi_k}/\bar{\alpha}_k$ = energy flux
$\bar{\zeta}_k^{Re}$ $(\overline{\chi_k\rho_k q'_k e'_k} + \overline{\chi_k\rho q'_k} - \overline{\chi_k\tau\cdot q'_k} + \overline{\chi_k\rho_k q'_k q'^2_k/2})/\bar{\alpha}_k$ = turbulent energy flux

Cross-sectional area averaged quantities

$\langle\cdot\rangle$ cross-sectional area averaging operator
$A(x)$ channel cross-sectional area
α_k $\langle\bar{\alpha}_k\rangle$ = volume fraction
α_{kw} $\dfrac{D}{4A}\oint_C \dfrac{\bar{\alpha}_k}{N}\,ds$ = wall volume fraction
C_{ek} $\langle\bar{\alpha}_k\bar{\rho}_k\bar{q}_k(\bar{e}_k + \bar{e}_k^{Re} + \bar{q}_k^2/2)\rangle\cdot e_x/(\alpha_k\rho_k u_k E_k)$ = energy profile parameter
C_{ss} shear stress profile parameter
C_{uk} $\langle\bar{\alpha}_k\bar{\rho}_k\bar{q}_k\bar{q}_k\rangle\cdot e_x\cdot e_x/\alpha_k\rho_k u_k^2$ = momentum profile parameter
D $4A/\int_{C_w} ds$ = effective channel diameter (C_w = perimeter in contact with mixture)
E_k $e_k + e_k^{Re} + u_k^2/2$ = total energy
e_k $\langle\bar{\alpha}_k\bar{\rho}_k\bar{e}_k\rangle/\alpha_k\rho_k$ = internal energy
e_{ki} $\langle\bar{e}_{ki}\Gamma_k\rangle/\Gamma_k$ = interfacial internal energy
e_k^{Re} $\langle\bar{\alpha}_k\bar{\rho}_k(\bar{e}_k^{Re} + \frac{1}{2}q'^2_k)\rangle/\alpha_k\rho_k$ = turbulent kinetic energy
f_{mk} $\langle\bar{f}_k\rangle$ = bulk mass source
f_{pk} $\langle\bar{\alpha}_k\bar{\rho}_k f_{pk}\rangle\cdot e_x/\alpha_k\rho_k$ = bulk momentum source
F_{Fax} Faxen force
F_{Bas} Basset force
F_D drag force
F_{vm} virtual mass force
F_L lift force
G_k $\langle\bar{G}_k\rangle$ = interfacial energy source
Γ_k $\langle\bar{\Gamma}_k\rangle$ = mass generation rate
M_k $\langle\bar{M}_k\rangle\cdot e_x$ = interfacial force
M'_k $\langle\bar{M}'_k\rangle\cdot e_x$ = added interfacial forces
p_k $\langle\bar{\alpha}_k\bar{p}_k\rangle/\alpha_k$ = pressure
p_{ki} interface pressure
r_k $\langle\bar{\alpha}_k\bar{\rho}_k\bar{r}_k\rangle/\alpha_k\rho_k$ = heating source
ρ_k $\langle\bar{\alpha}_k\bar{\rho}_k\rangle/\alpha_k$ = density
T_k $\langle\bar{\alpha}_k\bar{T}_k\rangle\cdot e_x\cdot e_x/\alpha_k$ = stress
T_k^{Re} $\langle\bar{\alpha}_k\bar{T}_k^{Re}\rangle\cdot e_x\cdot e_x/\alpha_k$ = Reynolds stress
T_{kw} $\dfrac{1}{A\alpha_{kw}}\oint_C \dfrac{\bar{\alpha}_k(\bar{T}_k\cdot n)\cdot e_x}{N}\,ds$ = wall stress
τ_k $\langle\bar{\tau}_k\rangle\cdot e_x\cdot e_x/\bar{\alpha}_k$ = shear stress
τ_{kw} wall shear stress
u_k $\langle\bar{\alpha}_k\bar{\rho}_k\bar{q}_k\rangle\cdot e_x/\alpha_k\rho_k$ = axial velocity
$u_{ki}^2/2$ $\langle\bar{q}_{ki}^2\cdot\bar{\Gamma}_k/2\rangle/\Gamma_k$ = interfacial kinetic energy
u_{ki} $\langle\bar{q}_{ki}\bar{\Gamma}_k\rangle\cdot e_x/\Gamma_k$ = interfacial velocity
W_k $\langle\bar{W}_k\rangle$ = interfacial work
ξ_h heated channel perimeter
ζ_k $\langle\bar{\alpha}_k\bar{\zeta}_k\rangle\cdot e_x/\alpha_k$ = axial energy flux
ζ_k^{Re} $\langle\bar{\alpha}_k\bar{\zeta}_k^{Re} - \bar{T}_k\cdot q'_k\rangle\cdot e_x/\alpha_k$ = turbulent axial energy flux
ζ_{kw} $\dfrac{1}{\xi_h}\oint_C \dfrac{\bar{\alpha}_k\bar{\zeta}_k\cdot n}{N}\,ds$ = wall energy flux

Quantities used in hyperbolicity analysis

c sound speed in gas phase
C_{vm} virtual mass coefficient
C_D drag coefficient
C_s interfacial pressure coefficient
d_L laminar energy friction factor
d_T turbulent energy friction factor
Δ discriminant of eigenvalue equation
λ eigenvalue of conservation laws
q $\alpha_2\rho_1/\alpha_1\rho_2$
R ρ_1/ρ_2 = density ratio
ϕ_T fluctuation term coefficient
Φ $V^2\alpha_2\phi_T$
T $1 - R - 1/\alpha_1$
V $(u_2 - u_1)/c$
W $V^2 d_L(1 - \gamma)\alpha_2/\alpha_1$

References

1 Hancox, W. T., Ferch, R L., Liu, W. S , and Nieman, R E. One-dimensional models for transient gas–liquid flows in ducts *Int. J Multiphase Flow* 1980, **6**, 25–40

2 Prosperetti, A. and Van Wijngaarden, L. On the characteristics of the equations of motion for a bubbly flow and the related problem of critical flow *J. Eng. Math.* 1976, **10**, 153–162

3 Soo, S. L. *Fluid Dynamics of Multiphase Systems* Ginn, Blaisdell, 1967

4 Gough, P. S. and Zwarts, F. J. Modeling Heterogeneous Two-Phase Reacting Flow. *AIAA J.* 1979, **17**, 17–25

5 Gidaspow, D Modeling of two-phase flow. Round table discussion (RT-1-2) *Proc 5th Int Heat Transfer Conf* VII, 1974, pp. 163–164

6 Fitt, A. D Mixed hyperbolic-elliptic systems in industrial problems. *Proc. ECMI88,* eds J. Manley, S McKee, and D Owens, Strathclyde, Teubner, 1988, pp. 205–214

7 Stewart, H. B. and Wendroff, B. Two-phase flow: models and methods, review article. *J. Comp. Phys.* 1984, **56**, 363–409

8 Stuhmiller, J H. The influence of interfacial pressure forces on the character of two-phase flow model equations *Int J Multiphase Flow* 1977, **3**, 551–560

9 Ransom, V. H and Hicks, D. L. Hyperbolic two-pressure models for two-phase flow. *J Comp Phys* 1984, **53**, 124–151

10 Drew, D. A. Averaged field equations for two-phase media *Stud Appl. Math.* 1971, **50**, 133–166

11 Ishii, M. *Thermo-fluid Dynamic Theory of Two-Phase Flows* Paris, Eyrolles, 1975

12 Drew, D. A and Lahey, R T. The application of general constitutive principles to the derivation of multidimensional two-phase flow equations *Int J Multiphase Flow* 1979, **5**, 243–264

13 Drew, D. A. Mathematical modelling of two-phase flow *Ann Rev. Fluid Mech.* 1983, **15**, 261–291

14 Drew, D. A and Wood, R. T. *Overview and Taxonomy of Models and Methods for Workshop on Two-Phase Flow Fundamentals* National Bureau of Standards, Gaithersburg, MD, 1985

15 Drew, D. A , Cheng, L , and Lahey, R T The analysis of virtual mass effects in two-phase flow *Int J Multiphase Flow* 1979, **5**, 233–242

16 Cook, T. L and Harlow, F. H. Virtual mass in multiphase flow. *Int J Multiphase Flow* 1984, **10**, 691–696

17 Drew, D. A. Two-phase flows: constitutive equations for lift and Brownian motion of some basic flows *Arch Rational Mech. Anal.* 1976, **62**, 149–163

18 Fitt, A. D. The numerical and analytical solution of ill-posed systems of conservation laws *Appl Math Modelling* 1989, **13**, 618–631

19 Fitt, A. D. A rigorous derivation of a set of two-dimensional equations for gas/particulate flow in a channel. CIT Mathematics & Ballistics Group Report MB 1/87, 1987

20 Biesheuvel, A. and Gorissen, W. C M. Void fraction disturbances in a uniformly bubbly fluid *Int. J Multiphase Flow* 1990, **16**, 211–231

21 Hunt, F R. W. *Internal Ballistics* His Majesty's Stationary Office, London, 1951

22 Krier, H., T'ien, J. S., Sirignano, W. A., and Summerfield, M. Nonsteady burning phenomena of solid propellants: theory and experiments *AIAA J.* 1968, **6**, 278–285

23 Krier, H., Rajan, S., and Van Tassell, W. F. Flame-spreading and combustion in packed beds of propellant grains *AIAA J* 1976, **14**, 301–309

24 Hoffman, S. J and Krier, H. Fluid Mechanics of Deflagration-to-Detonation Transition in Porous Explosives and Propellants. *AIAA J* 1981, **19**, 1571–1579

25 Gough, P S. On the closure and character of the balance equations for heterogeneous two phase flow. Dynamics and modelling of reactive systems, Seminar presented at the University of Wisconsin—Madison, 1979

26 Batchelor, G. K. *An Introduction to Fluid Dynamics* Cambridge University Press, 1985

27 Van Beek, P. A counterpart of Faxen's formula in potential flow. *Int J. Multiphase Flow* 1985, **11**, 873–879

28 Geurst, J. A. Virtual mass in two-phase bubbly flow *Physica* 129A 1985, 233–261

29 Fitt, A. D. Symbolic computation of hyperbolicity regions for systems of two-phase flow conservation laws using MAPLE *J Symbolic Comput.* 1989, **8**, 305–308

30 Barnard, S and Child, J M *Higher Algebra* Macmillan, London, 1965

31 Nigmatulin, R. Spatial averaging in the mechanics of heterogeneous and dispersed systems *Int J Multiphase Flow* 1979, **5**, 353–386